



HAL
open science

AAV8 locoregional delivery induces long-term expression of an immunogenic transgene in macaques despite persisting local inflammation

Gwladys Gernoux, Mickaël Guilbaud, Marie Devaux, Malo Journou, Virginie Pichard, Nicolas Jaulin, Adrien Léger, Johanne Le Duff, Jack-Yves Deschamps, Caroline Le Guiner, et al.

► To cite this version:

Gwladys Gernoux, Mickaël Guilbaud, Marie Devaux, Malo Journou, Virginie Pichard, et al.. AAV8 locoregional delivery induces long-term expression of an immunogenic transgene in macaques despite persisting local inflammation. *Molecular Therapy - Methods and Clinical Development*, 2021, 20, pp.660 - 674. 10.1016/j.omtm.2021.02.003 . inserm-03172941

HAL Id: inserm-03172941

<https://inserm.hal.science/inserm-03172941>

Submitted on 18 Mar 2021

HAL is a multi-disciplinary open access archive for the deposit and dissemination of scientific research documents, whether they are published or not. The documents may come from teaching and research institutions in France or abroad, or from public or private research centers.

L'archive ouverte pluridisciplinaire **HAL**, est destinée au dépôt et à la diffusion de documents scientifiques de niveau recherche, publiés ou non, émanant des établissements d'enseignement et de recherche français ou étrangers, des laboratoires publics ou privés.



Distributed under a Creative Commons Attribution - NoDerivatives 4.0 International License

AAV8 locoregional delivery induces long-term expression of an immunogenic transgene in macaques despite persisting local inflammation

Gwladys Gernoux,¹ Mickaël Guilbaud,¹ Marie Devaux,¹ Malo Journou,¹ Virginie Pichard,¹ Nicolas Jaulin,¹ Adrien Léger,¹ Johanne Le Duff,¹ Jack-Yves Deschamps,³ Caroline Le Guiner,¹ Philippe Moullier,¹ Yan ChereI,² and Oumeya Adjali¹

¹Université de Nantes, CHU de Nantes, INSERM UMR 1089, Translational Gene Therapy for Genetic Diseases, 44200 Nantes, France; ²INRA UMR 703, PAnTher, ONIRIS, 44307 Nantes, France; ³Centre de Boisbonne, ONIRIS, 44307 Nantes, France

Adeno-associated virus (AAV) vectors are considered efficient vectors for gene transfer, as illustrated by recent successful clinical trials targeting retinal or neurodegenerative disorders. However, limitations as host immune responses to AAV capsid or transduction of limited regions must still be overcome. Here, we focused on locoregional (LR) intravenous perfusion vector delivery that allows transduction of large muscular areas and is considered to be less immunogenic than intramuscular (IM) injection. To confirm this hypothesis, we injected 6 cynomolgus monkeys with an AAV serotype 8 (AAV8) vector encoding for the highly immunogenic GFP driven by either a muscle-specific promoter (n = 3) or a cytomegalovirus (CMV) promoter (n = 3). We report that LR delivery allows long-term GFP expression in the perfused limb (up to 1 year) despite the initiation of a peripheral transgene-specific immune response. The analysis of the immune status of the perfused limb shows that LR delivery induces persisting inflammation. However, this inflammation is not sufficient to result in transgene clearance and is balanced by resident regulatory T cells. Overall, our results suggest that LR delivery promotes persisting transgene expression by induction of Treg cells *in situ* and might be a safe alternative to IM route to target large muscle territories for the expression of secreted therapeutic factors.

INTRODUCTION

Recombinant adeno-associated virus (rAAV) is now considered an efficient and successful gene therapy vector, as illustrated by recent US Food and Drug Administration (FDA) and European Medicines Agency (EMA) approvals for the treatment of neurodegenerative, retinal, or metabolic disorders.^{1–3} This vector also showed great promises for the treatment of muscular dystrophies, including Duchenne muscular dystrophy (DMD)^{4,5} or limb-girdle muscular dystrophy type 2D (LGM2D).^{6,7} At first, some of these clinical trials used the intramuscular (IM) route for vector delivery, but this mode of administration showed some limits. Actually, IM delivery does not allow to achieve therapeutic efficacy due to transduction of limited regions and is often associated with immune responses to the vector

and/or the transgene product in animal models and patients.^{8–14} The intravenous (i.v.) route is currently used for these disorders in several clinical trials (NCT03368742,¹⁵ NCT03375164,¹⁶ and NCT03362502¹⁷ [DMD] and NCT03199469¹⁸ [X-linked myotubular myopathy (XLMTM)]) but requires high vector doses (up to 3e14 viral genomes/kilogram [vg/kg]) to achieve a therapeutic effect that might lead to liver dysfunction, as recently described in nonhuman primates (NHPs)¹⁹ but also in 3 XLMTM patients,²⁰ or to renal impairment, as observed in 1 DMD patient.²¹ These adverse events were attributed to an activation of the innate system post-dosing. As an alternative, the locoregional (LR) i.v. perfusion can be used to target large muscle territories. This method consists of transiently isolating the limb from the general circulation using an atraumatic tourniquet. The vector is then injected under pressure, allowing rAAV extravasation in the limb, leading to transduction of large areas, as described in dogs and NHPs after a single LR injection.^{22–24}

Interestingly, the LR delivery is considered more efficient and less immunogenic than the IM route.^{25,26} Our group and others reported that LR delivery is (1) well tolerated,^{27,28} (2) allows sustained transgene expression^{25,29,30} in animal models, and (3) results in a better vector distribution in muscles compared to IM delivery.^{23,28} More importantly, we recently showed that LR delivery of a rAAV1 allows long-term transgene expression up to 5 years post-dosing in NHPs without any immune response to the transgene product and in absence of any immune-suppressive regimen,²⁶ although, in this previous study, we used a rAAV1 known to present limited vector spreading, a muscle-specific desmin promoter to limit gene expression in muscle cells, and a low dose of vector (1e11 vg/kg). All these factors (serotype, dose, and promoter) may explain why we did not observe an immune response to the transgene product.

Received 27 August 2020; accepted 3 February 2021;
<https://doi.org/10.1016/j.omtm.2021.02.003>.

Correspondence: Oumeya Adjali, Université de Nantes, CHU de Nantes, INSERM UMR 1089, Translational Gene Therapy for Genetic Diseases, 22 Bd Benoni Goullin, 44200 Nantes, France.

E-mail: oumeya.adjali@univ-nantes.fr



Table 1. Experimental groups

Animal	Vector	Promotor	Mode of delivery	Dose (vg/kg)	Endpoint (months)
Mac 1	scAAV2/8-GFP	desmin	LR	7e12	13
Mac 2	scAAV2/8-GFP	desmin	LR	7e12	12
Mac 3	scAAV2/8-GFP	desmin	LR	7e12	9
Mac 4	scAAV2/8-GFP	CMV	LR	7e12	12
Mac 5	scAAV2/8-GFP	CMV	LR	7e12	12
Mac 6	scAAV2/8-GFP	CMV	LR	7e12	1
Ctrl IM	scAAV2/8-GFP	CMV	IM	7e12	14

IM, intramuscular; LR, locoregional intravenous delivery; vg/kg, viral genome/kilogram

To confirm and understand the low immunogenicity of the LR delivery and its ability to induce long-term transgene expression in cynomolgus monkeys, we challenged this administration route by using more immunogenic conditions and an AAV serotype 8 (AAV8) that is (1) less seroprevalent than AAV1, (2) used to target muscles for the secretion of therapeutic factors,^{28,31} and (3) used in clinical trials.¹⁸ We chose to work with a higher dose (7e12 vg/kg) of a self-complementary (sc) instead of a single-stranded (ss) rAAV8 vector, a setting described to be more immunogenic.^{32,33} The sc rAAV8 vector used encodes for the green fluorescent protein (GFP) reported to be highly immunogenic in large animal models.^{34,35} We also tested a tissue-specific desmin promoter (n = 3) versus an ubiquitous cytomegalovirus (CMV) promoter (n = 3).

Here, we described that, even under highly immunogenic conditions, LR delivery of rAAV in cynomolgus monkeys induced long-term transgene expression. Surprisingly, the GFP expression was maintained up to 1 year post-dosing, despite a peripheral anti-transgene humoral response and a GFP-specific CD8 T cell response. This peripheral response was associated with the detection of muscle-infiltrated cells, including CD4 T cells and CD8 T cells but more importantly regulatory T cells (Tregs). An in-depth analysis of the immune status of the injected limb at early (day 7 to day 90) and long-term (up to 1 year) time points post-injection showed that rAAV LR injection leads to persisting expression of inflammatory signals. These signals in addition to GFP expression seem to mimic a chronic inflammation that would be regulated by Tregs *in situ*. Overall, these data confirm that LR delivery induces long-term expression of the transgene without inducing a deleterious T cell response.

RESULTS

Locoregional delivery allows long-term GFP expression in perfused limb

In contrast to the IM route, LR administration of an AAV vector leads to long-term transgene expression, as reported by our group and

others.^{24–26,29} To confirm that this mode of delivery is less immunogenic, we injected 6 monkeys with a sc rAAV8 vector encoding for the GFP described to be highly immunogenic in NHPs.^{34,35} The expression of the GFP was driven by a desmin muscle-specific promoter (n = 3) or a CMV ubiquitous promoter (n = 3; Table 1). All monkeys received a dose of 7e12 vg/kg and were followed for up to 1 year except for Mac 6. This monkey showed a pain in the perfused limb, probably due to a higher LR-induced vector extravasation and subsequent high level of GFP expression described to be toxic in monkeys.^{34,36} Therefore, for ethical reasons, this animal was euthanized at 1 month post-dosing. The vector biodistribution was analyzed by quantitative PCR (qPCR) in perfused and contralateral limbs (Figure 1A). As previously described after LR delivery, the analysis showed a broad biodistribution of the vector in the injected limb with 0.01 to 1 vg per diploid genome (vg/dg), depending on the muscle analyzed. Higher vector copy numbers were detected in Mac 6 muscles with 2.2 vg/dg in the tibialis and up to 20 vg/dg in the gastrocnemius muscle, but the tissues were collected at 1 month post-dosing in contrast to the other monkeys. The statistical analysis did not show a significant difference between the NHPs (Mann-Whitney test). As expected, vector genomes were detected in contralateral muscles but at lower levels (between 0.01 and 0.29 vg/dg) and also in peripheral organs (including liver, spleen, and inguinal lymph nodes; not shown), an observation that is probably due to the release of the tourniquet. In addition to the vector biodistribution, the GFP expression was analyzed by immunostaining in the perfused limb over time (Figure S1) and at necropsy (Figure 1B). The GFP was detected at day 30 and persisted up to 1 year post-dosing in all monkeys injected with either desmin or CMV promoters. GFP relative expression was also detected by qRT-PCR in the contralateral limb (not shown). As anticipated, the intensity of transgene expression was higher in the CMV group compared to the desmin group.

Sustained transgene expression despite humoral and cellular responses to the transgene product

In our previous studies, we reported a persisting transgene expression after LR delivery without detection of an anti-transgene immune response.^{25,26} To confirm these results, we also analyzed the immune response to the transgene product in our model by assessing humoral and cellular immune responses to the GFP (Table 2). Surprisingly, and in contrast to our previous model, we detected in all monkeys high titers of anti-GFP immunoglobulin G (IgG) antibodies (titer > 327,680; Table S1) and an interferon- γ (IFN- γ)-positive response when peripheral blood mononuclear cells (PBMCs) collected at different time points post-dosing were restimulated with an overlapping peptide library spanning the GFP sequence with a response observed earlier for the CMV promoter compared to the desmin (day 14 versus day 45, respectively; data not shown). To understand the fact that GFP expression persisted over time despite the induction of a specific host immunity, we characterized this immune response. We first investigated whether the cellular response was mediated by either CD8 or CD4 T cells. To do so, an IFN- γ ELISpot assay was performed on total, CD4-depleted, and CD8-depleted splenocytes isolated at day 60 post-dosing (Table 2; Figure 2). The efficiency of

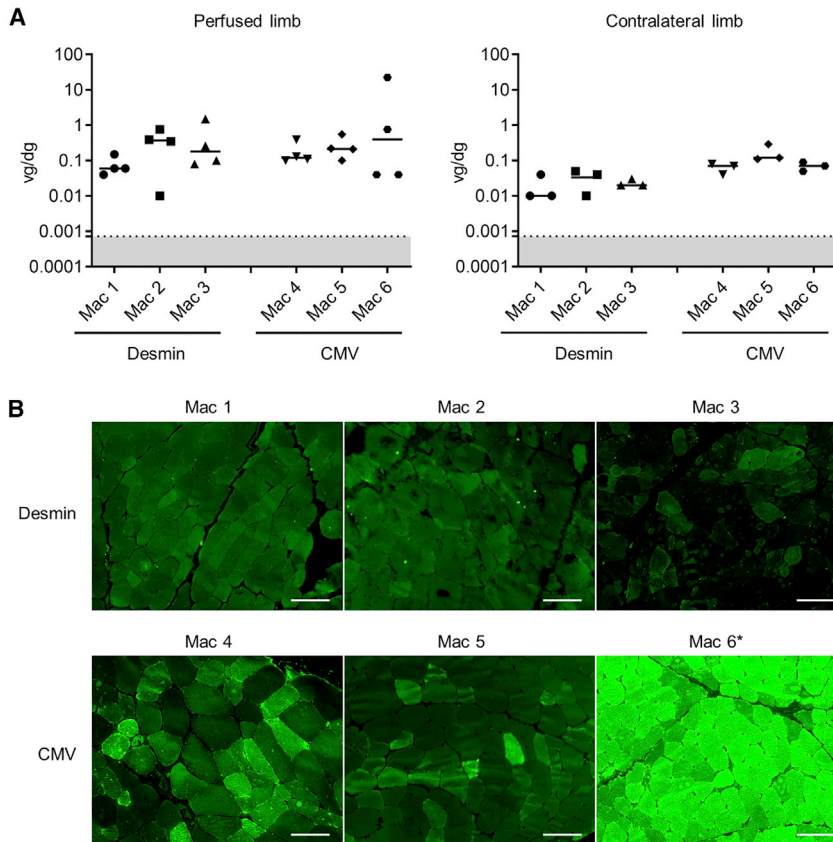


Figure 1. GFP expression in perfused limb up to 1 year post-injection

Nonhuman primates were injected LR with a scAAV8-Des-GFP ($n = 3$) or a scAAV8-CMV-GFP vector ($n = 3$) (7×10^{12} vg/kg). Muscles were harvested at necropsy. (A) Detection of viral genome by qPCR in muscles from perfused limb (4 muscles are represented for each animal) and from contralateral limb (3 muscles are represented for each animal). vg/dg, viral genome/diploid genome. Lines represent the median. The dotted line represents the qPCR limit of quantification (0.0007 vg/dg). No significant statistical difference is observed between the nonhuman primates (Mann-Whitney test). (B) GFP expression in perfused limb determined by immunostaining is shown. Scale bar: 100 μm . *Mac 6 was euthanized 30 days after dosing.

each depletion was evaluated by flow cytometry (Figure 2A). These depletions showed that all the animals developed a specific anti-GFP T cell response mediated by CD8 T cells (e.g., by CD4-depleted splenocytes) except for Mac 2. Results obtained on total splenocytes confirmed the results obtained on PBMCs at necropsy (Table 2; Figure 2B). To further determine whether this cellular immunity was a conventional effector CD8 T cell response, we performed an interleukin-2 (IL-2) ELISpot assay on splenocytes isolated at day 60 post-injection as well (Table 2). IL-2 was not secreted by neither total splenocytes, CD4, nor CD8 T cells after GFP stimulation, except for Mac 2. The absence of IL-2 secretion in response to transgene peptide stimulation suggests that CD8 T cell response could not be conventional, as IL-2 is usually described to promote CD8 effector response.^{37,38}

Detection of regulatory T cells in the perfused limb

A recent study suggested that, in animal models, the characterization of muscle-infiltrated cells following rAAV delivery would be more relevant than the analysis of peripheral immune response to understand the absence of a deleterious T cell response.³⁹ Therefore, we performed a hematoxylin-phloxin-saffron (HPS) staining on perfused and contralateral muscles sections to analyze the presence of mononuclear cell infiltrates. Muscle-infiltrated cells were detected in all monkeys up to 12 months post-injection in perfused limb (Figure 3A),

but not in contralateral limb (Figure S2). In the perfused limb, we noticed these cell infiltrates and some centranucleated fibers, suggesting a possible muscle regeneration. However, no harmful inflammation was observed because viral genomes are still detected at necropsy (Figure 1A). During regular clinical examinations, we did not observe any muscle wasting in any monkey over time. To verify that mononuclear cell infiltrates were not associated to fibrosis or adiposis, we performed a picrosirius red staining. A localized fibrosis was detected in the perimysium in perfused limb in all monkeys but was comparable to muscle collected on an uninjected control

monkey (Figure S3), suggesting it was not related to gene transfer. An in-depth characterization of muscle-infiltrated cells by immunohistochemistry showed the presence of both CD3+ CD4+ T cells and CD3+ CD8+ T cells (Figures 3B and 3C, respectively). Sustained transgene expression despite the detection of CD4 and CD8 T cells in addition to a transgene-specific peripheral immune response suggests the initiation of an immune modulation mechanism *in situ*. Two cell populations responsible for the absence of a deleterious immune response have been described in AAV gene transfer: regulatory T cells (CD3+CD4+FoxP3+ cells) and exhausted T cells (CD3+CD8+PD-1+).^{39–41} In this study, we performed an immunostaining on muscle collected at necropsy to verify the presence of these cells in the injected limb to explain long-term GFP expression. Infiltrated regulatory T cells (CD4+Foxp3+ cells; Figure 4) but no exhausted T cells (CD3+PD1+ cells; Figure S4) were detected *in situ* after 1 year post-injection in both desmin and CMV groups.

Inflammatory signals are delivered in injected limb up to 1 year post-vector administration

Because we observed a peripheral immune response and muscle-infiltrated cells, including Tregs up to 1 year post-dosing, we wanted to further study the immune status of the perfused limb. To do so, we quantified the expression of 84 genes involved in inflammatory response, including cytokines, chemokines, and receptors. For all

Table 2. Humoral and cellular immune responses to GFP

		Anti-GFP IgG antibodies		PBMCs		Splenocytes					
		Baseline	Necropsy	IFN- γ secretion to GFP		IFN- γ secretion to GFP			IL-2 secretion to GFP		
				Baseline	Necropsy	Total	CD4-depleted	CD8-depleted	Total	CD4-depleted	CD8-depleted
Desmin	Mac1	-	+	-	+	+	+	-	-	-	-
	Mac 2	-	+	-	+	+	+	+	+	-	+
	Mac 3	-	+	-	+	+	+	-	-	-	-
CMV	Mac 4	-	+	-	+	+	+	-	-	-	-
	Mac 5	-	+	-	+	+	+	-	-	-	-
	Mac 6	-	N/A	-	N/A	N/A	N/A	N/A	N/A	N/A	N/A

IgG, immunoglobulin; IFN- γ , interferon-gamma; IL-2, interleukin-2; N/A, not applicable; PBMCs, peripheral blood mononuclear cells; -, no response; +, positive response

monkeys, 4 muscles (2 from the perfused limb and 2 from the contralateral limb) were analyzed at 4 time points (day 7, 1 month, 3 months, and at necropsy). Relative quantification (RQ) for each gene has been determined by qRT-PCR and reported on a heatmap (Figure 5A and <https://adrienleger.com/TaqMDA/> for analysis on each monkey). At day 7 post-injection, we did not observe noticeable differences in term of gene expression between the perfused limb and the contralateral limb (Figure 5A). On the contrary, our analysis showed, at 1 month post-injection, an upregulation of inflammatory genes in the perfused limbs of all NHPs compared to contralateral limbs, with no difference between the two desmin and CMV promoters. This upregulation persisted until up to 1 year for all monkeys (Figure 5A). Then, we performed a principal-component analysis (PCA) based on these relative quantification data (Figure 5B and <https://adrienleger.com/TaqMDA/> for analysis on each monkey). The inflammatory gene expression pattern in contralateral limb at all time points and in the perfused limb at day 7 were found grouped together. This indicates there is no noticeable differences between the contralateral limb and the day 7 time point. On the other hand, the inflammatory gene expression pattern in muscles collected on the perfused limb at 1 month, 3 months, and at necropsy were clearly opposed on the first principal component to the control group (e.g., contralateral limb). This confirms the pattern obtained in the heatmap-based analysis with the initiation of inflammatory gene expression after LR rAAV delivery starting from at least 1 month and lasting up to 1 year post-dosing. Finally, from the variable diagram generated with the PCA (Figure S5 and <https://adrienleger.com/TaqMDA/> for analysis on each monkey), we quantified the number of upregulated inflammatory genes at each time point. These data were compared to the results obtained on a control monkey injected intramuscularly (Ctrl IM) with the same scAAV8-CMV-GFP vector and at the same dose (7e12 vg/kg; Figure 5C). We observed that the number of upregulated genes in the injected muscle of the Ctrl IM monkey increased and reached a peak at 1 month post-dosing and then this number decreased between 1 and 3 months (from 45 overexpressed genes to less than 20). After 3 months, the number of overexpressed genes returned to levels comparable to day 7 time point, and this was correlated to the loss of transgene expression that was observed in this con-

trol IM animal at 3 months post-dosing (Figure S6). In contrast, for all monkeys injected by LR route (either desmin or CMV group), the number of upregulated genes in the perfused limb increased between day 7 and 3 months post-dosing and then decreased but remained noticeable until necropsy. Genes involved in inflammatory response consistently upregulated at 3 months for monkeys injected LR and at 1 month for Ctrl IM monkey have been reported in Table 3 and led to a panel of 21 cytokines. Surprisingly, the panel is the same between the Ctrl IM monkey who cleared the transgene after 3 months in the muscle and the monkeys injected LR with either the desmin or the CMV promoter, who were still expressing the GFP protein after 1 year. Thus, the major difference is related to the kinetic that is different between the 2 modes of delivery with a delayed upregulation and persistence of inflammatory gene expression up to 1 year in the LR groups (Figure 5C). This difference can be explained by LR delivery, resulting in a broad transduction of muscles in the entire limb with more transduced muscles but less viral genome numbers per cell compared to the IM route, where viral genomes are concentrated at the site of injection. After LR delivery, it may take more time to have a sufficient amount of GFP *in situ* to induce inflammatory signals.

DISCUSSION

So far, the major limit described in patients treated with AAV vectors in clinical trials is the host immune response. The initiation of an immune response to the capsid and/or the transgene product has been described in clinical trials targeting metabolic, neurodegenerative, and neuromuscular disorders.^{8,14,31,42-45} Several factors can modulate the initiation of an immune response: among them, the vector dose, the promoter, the transgene, and/or the administration route of the product.⁴⁶ AAV-mediated muscle gene transfer using i.v. delivery necessitates high vector doses and showed adverse events in patients due to the reactivation or initiation of a cytotoxic T cell response to the capsid that are now managed by transient corticosteroid-based immunosuppressive treatments. As an alternative to the systemic route, we focused on the LR delivery. This alternative administration route is of great interest for muscle-directed gene transfer to treat metabolic disorders, because it allows transduction of large muscle

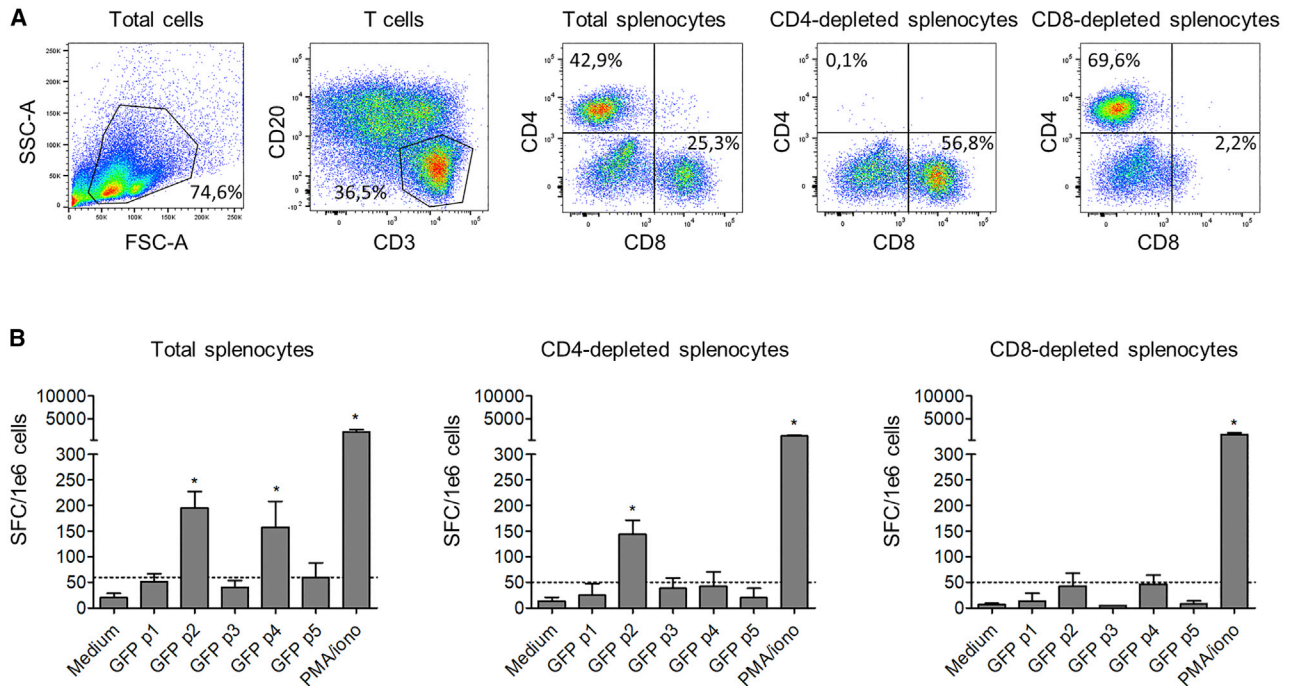


Figure 2. IFN- γ secretion to GFP is mediated by CD8 T cells

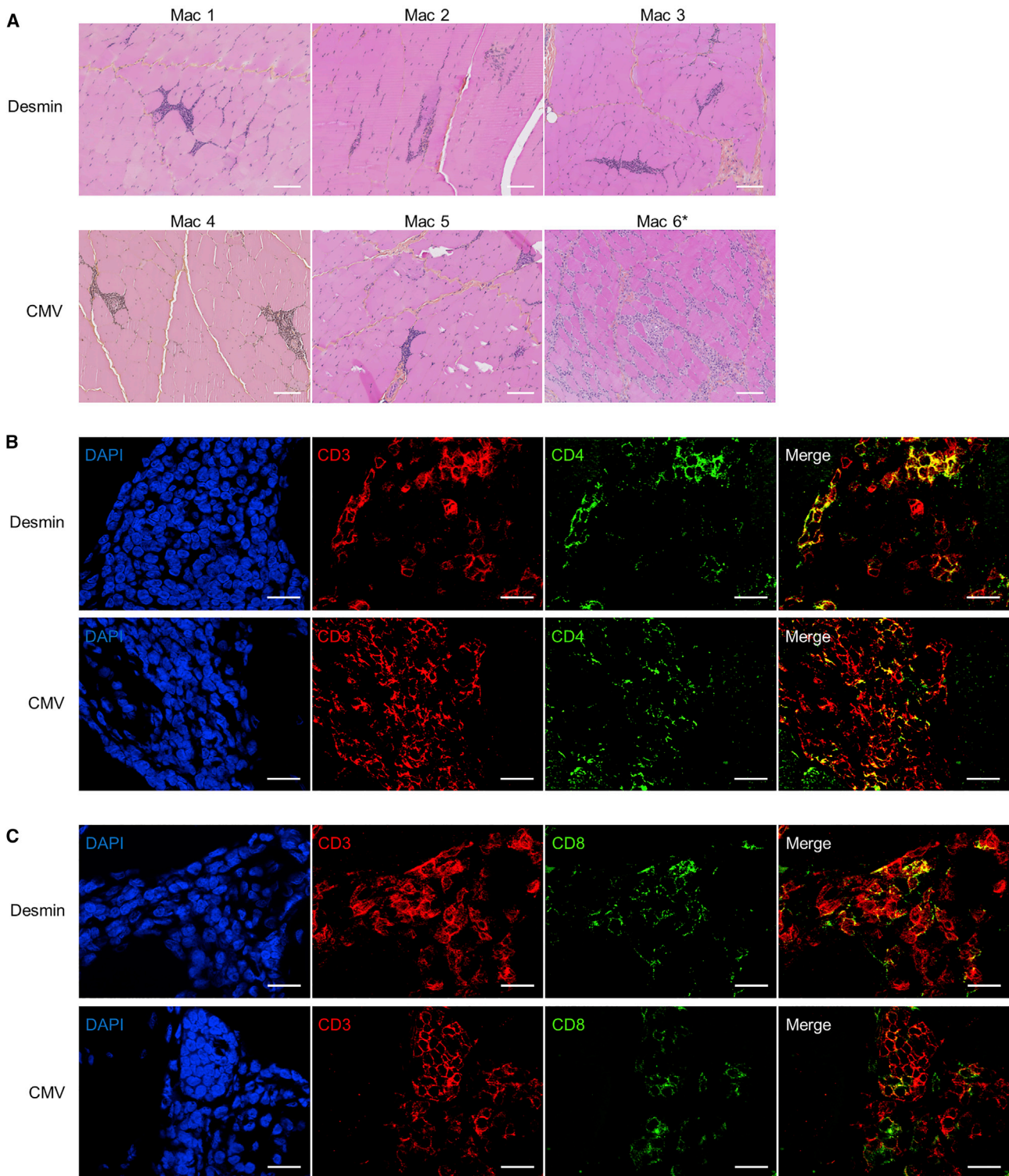
Spleens were harvested at day 60 post-dosing, and splenocytes were isolated. (A) Cell depletion efficiency is shown. Percentages of CD4 (CD3+CD4+) and CD8 (CD3+CD8+) T cells were determined by flow cytometry before (total splenocytes) and after magnetic separation (CD4- and CD8-depleted splenocytes). (B) Total and CD4- and CD8-depleted splenocytes were stimulated *in vitro* with overlapping peptides (15 mers overlapping by 10 aas) spanning the GFP sequence (pool 1–5 [p1–p5]). Negative control consisted of unstimulated cells (medium alone), whereas PMA/ionomycin (PMA/iono) stimulation was used as a positive control for cytokine secretion. Responses were considered positive when the number of spot-forming colonies (SFCs) per 1e6 cells was >50 and at least 3-fold higher than the control condition (dotted line); asterisk (*) denotes positive response (DFR(2 \times) test). Error is represented as standard deviation (SD).

areas and release of therapeutic levels of secreted proteins. Moreover, it seems to not induce a deleterious immune response, at least to the transgene product. This mode of delivery was even described to be able to induce a transgene-specific tolerance mediated by IL-10-secreting FoxP3+CD4+ cells when a cyclophosphamide immune-suppressive regimen is administered.^{24–26,47} In the present study, we focused on the impact of a LR vector delivery to allow persisting transgene expression of an immunogenic protein. To confirm the low immunogenicity of this route, we injected in a relevant preclinical cynomolgus monkey model and in absence of any immune suppressive regimen a sc rAAV8 vector carrying the highly immunogenic GFP transgene at a relatively high dose (7e12 vg/kg). This dose range was previously reported to induce an immune response to either the GFP transgene product^{34,35} or the AAV capsid.^{14,40,42}

In our model, we confirmed that LR delivery of an AAV8 vector leads to persisting transgene expression, despite the high immunogenicity of its product. Surprisingly, and in contrast to previous studies, where either no response or only anti-transgene IgG responses were reported,^{26,29,47} we observed an anti-GFP cellular immune response. This response was detected at day 15 post-dosing in the CMV group versus at day 45 in the desmin group (not shown). The analysis in splenocytes showed that it was mediated by IFN- γ - and not IL-2-

secreting CD8 T cells. Secretion of IFN- γ by circulating cells not leading to loss of transgene expression is not unusual after rAAV delivery. It has already been described in previous clinical trials, where sustained transgene expression was explained by the presence of immune cells mediating tolerance (Tregs and/or exhausted T cells) that were detected in periphery or at the site of injection.^{39,41,48} In the present study, we analyzed the presence of muscle-infiltrating cells in the perfused limb at 1 year post-injection. We observed infiltration of CD4 and CD8 T cells but also T-reg cells that might explain persisting transgene expression. To understand long-term, muscle-infiltrated cells, we performed an in-depth analysis of the immune status of muscles collected in the perfused limb at early and late time points (from day 7 until 1 year post-dosing) by analyzing the expression of 84 genes involved in inflammatory response. Our results showed that expression of genes involved in inflammation increased between day 7 and 3 months post-dosing and persists until at least 1 year. These signals that are similar but persisting as compared to a control monkey injected IM may participate to the recruitment and persistence of the immune cells *in situ* and especially Tregs.

The presence of Tregs after rAAV delivery in the muscle has been described in alpha-1-antitrypsin-deficient-patients (AATD) and lipoprotein-deficient patients (LPL) who received an AAV1 vector



(legend on next page)

intramuscularly.^{39,41,48} The specificity of these Tregs was studied in AATD patients in periphery by restimulating PBMCs and showed that these Tregs were capsid specific; the expression of activation markers was observed only when PBMCs were stimulated with AAV peptides, not when they were stimulated with AAT peptides. The presence of these activated capsid-specific Tregs was explained by the persistence of AAV capsid in the injected muscle up to 1 year post-dosing.⁴¹ The main hypothesis was that long duration of AAV capsid antigen exposure was mimicking a chronic viral infection, leading to the induction of capsid-specific Tregs and exhausted T cells.^{39,41} In our cynomolgus preclinical model, the specificity of these Tregs (transgene product or capsid or both) remain to be characterized. Here, we did not detect a cellular immune response to the capsid in any animals, except Mac 4, that was already positive prior to vector delivery (Figure S7). But, as expected and previously described,^{14,36,39} all the animals showed anti-AAV8 neutralizing factors and IgG antibodies (not shown). The absence of an anti-capsid cellular immune response is not surprising because this response has not been anticipated in any preclinical model before translation of AAV-based strategies to patients.^{49,50} However, we observed comparable results to those described in AATD clinical trial when we assessed the peripheral immune response to the transgene product; we report long-term expression of GFP in monkeys that is correlated to Treg-infiltrating cells in the muscle, despite the detection of IFN- γ -secreting CD8 T cells. These findings might suggest that our Tregs are at least partially specific to the transgene product in our model.

Recruitment of Tregs at the site of inflammation is not only observed in the setting of chronic viral infection but also in some pathologies, including DMD, where the muscle is injured and the inflammation is chronic.^{51,52} In these diseases, Tregs play a role in cell homeostasis and control the extent of tissue damage by restraining the development of type 1 inflammatory response.⁵³ The depletion of Tregs has critical consequences; it leads to exacerbation of muscle inflammation^{53,54} and to the decrease of the expression of activation marker on M2 macrophages that have anti-inflammatory properties and are involved in tissue repair and remodeling phases.⁵⁵ In our model, LR delivery of an AAV8 vector leads to a long-term broad expression of a highly immunogenic protein in the perfused limb. The sustained inflammation related to the GFP might mimic a chronic inflammation and explain the recruitment and persistence of Tregs *in situ* up to 1 year post-dosing.

The analysis of the kinetic of the inflammatory gene expression supports this hypothesis and seems to be specific to the LR mode of delivery. Indeed, in our IM Ctrl monkey injected with the same AAV

vector via the IM route, we observed inflammation gene expression pattern comparable to an acute inflammation where immune cells infiltrate the muscle to clear necrotic muscle fibers. In this case, inflammatory cytokines are secreted to promote muscle stem cells proliferation and differentiation, which favor muscle regeneration.^{56,57} This phase lasts approximately 1 to 2 months.⁵⁸ In our study, after IM delivery, inflammatory genes are expressed no later than 3 months with a peak at 1 month post-dosing and are associated to a loss of transgene expression. Moreover, the analysis of vector biodistribution in the draining lymph node of this Ctrl IM monkey early after vector dosing (day 7) showed that 100 vg/dg are detected versus an average of 7.8 vg/dg in monkeys injected LR (Figure S8). This difference might result in higher antigen presentation to immune cells and delivery of danger signals after IM in contrast to the LR route, a finding that could contribute to the lower immunogenicity of the LR delivery. In addition to less viral genomes in the draining lymph node, after LR delivery, we observed inflammatory signals that persist over time and that are not sufficient to result in transgene clearance. We observed expression of chemokines that would explain recruitment of immune cells *in situ* and cytokines and their respective receptors that might participate to Treg induction or recruitment, including, but not limited to, (1) IL-10 receptor (IL-10R) that is critical to maintain suppressive function as it enables the generation and function of Tregs;^{59–61} (2) IFN- γ that may participate in induction of Foxp3 expression and conversion of CD4+CD25– T cells to CD4+ Tregs in an inflammatory environment;⁶² (3) tumor necrosis factor (TNF)/TNFR2 pathway, which is a key factor in maintaining sustained Foxp3 expression and function of Tregs, contributing to immune regulation in the inflammatory environment;^{63–65} and (4) IL-2R that is expressed by Tregs, for which IL-2 sensing is essential for survival, functional competency, and stability.^{66,67} Interestingly, some of these cytokines are also described in chronic inflammation,⁶⁸ supporting the hypothesis that GFP long-term expression might partially mimic this phenomenon. Importantly, none of the deleterious effects observed in case of chronic inflammation, including pain, muscle wasting, or fibrosis, have been observed in our model. We do observe some centrally nucleated fibers at 1 year post-injection in the injected limb (compared to the contralateral limb), which are usually associated with destruction and regeneration of muscle fibers. Because we observed a persistence of transgene expression, the presence of these fibers could rather be explained by the persisting inflammation. Actually, some cytokines upregulated in our model (Table 3), such as CCL2, described to contribute to the regeneration of muscle fibers or TNF- α responsible for the decrease of MyoD (myoblast determination protein 1) expression, which is a factor promoting muscle differentiation, might slow down or stop the

Figure 3. Detection of cellular infiltrates in the perfused limb after AAV8 delivery at necropsy

Nonhuman primates were injected LR with a scAAV8-Des-GFP (n = 3) or a scAAV8-CMV-GFP vector (n = 3; 7e12 vg/kg). Muscles were harvested at necropsy. (A) Infiltrated cell populations were analyzed by hematoxylin-phloxine-saffron staining in the perfused limb. Scale bar: 100 μ m. Mac 6 (*) was euthanized at 1 month post-dosing. (B) Detection of CD4 T cells (CD3+CD4+ cells) by immunohistochemistry in perfused limb is shown (Mac 2, Desmin; Mac 4, CMV). Each illustration is representative of each group. Scale bar: 20 μ m. (C) Detection of CD8 T cells (CD3+CD8+ cells) by immunohistochemistry in perfused limb is shown (Mac 3, Desmin; Mac 4, CMV). Each illustration is representative of each group. Scale bar: 20 μ m.

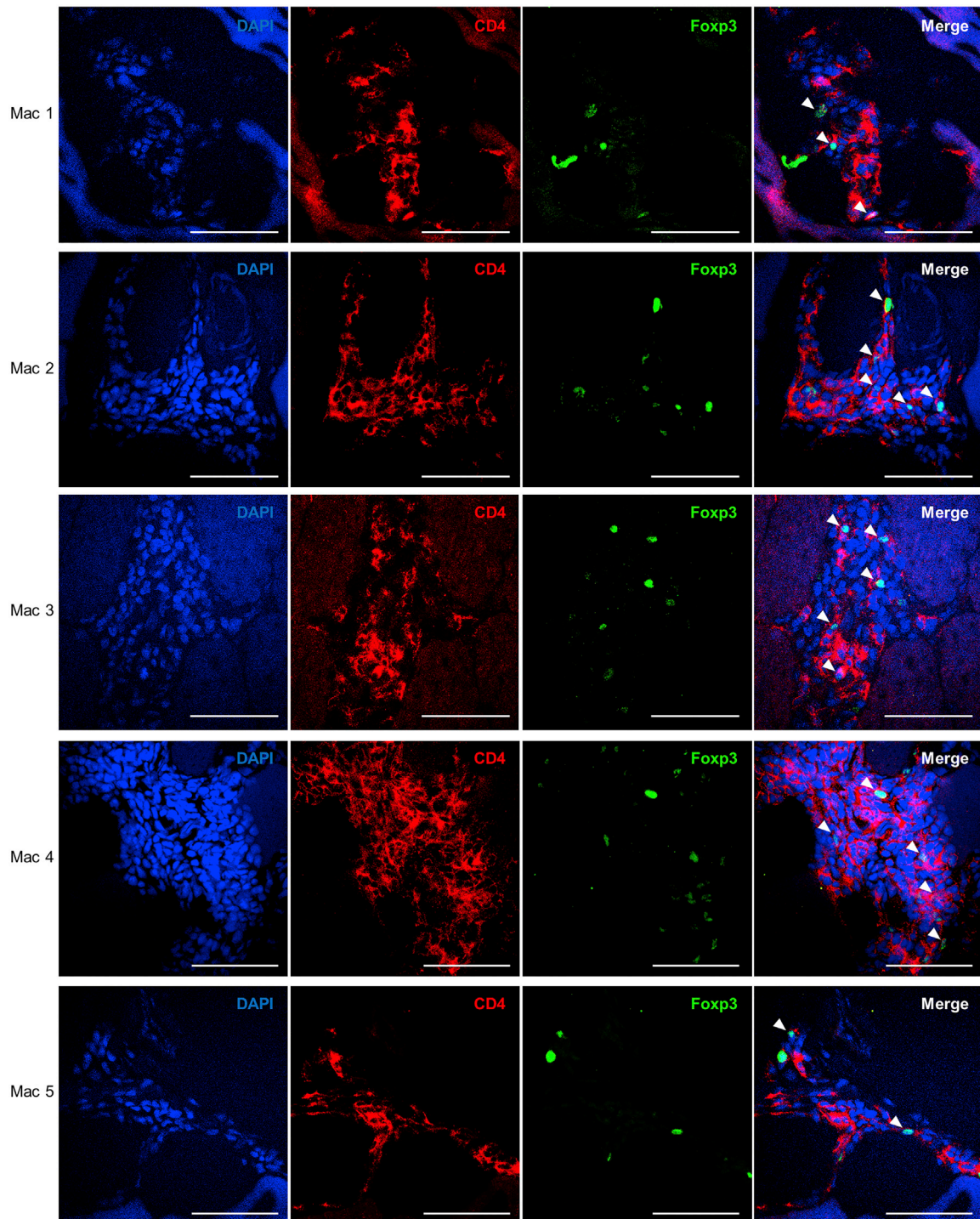
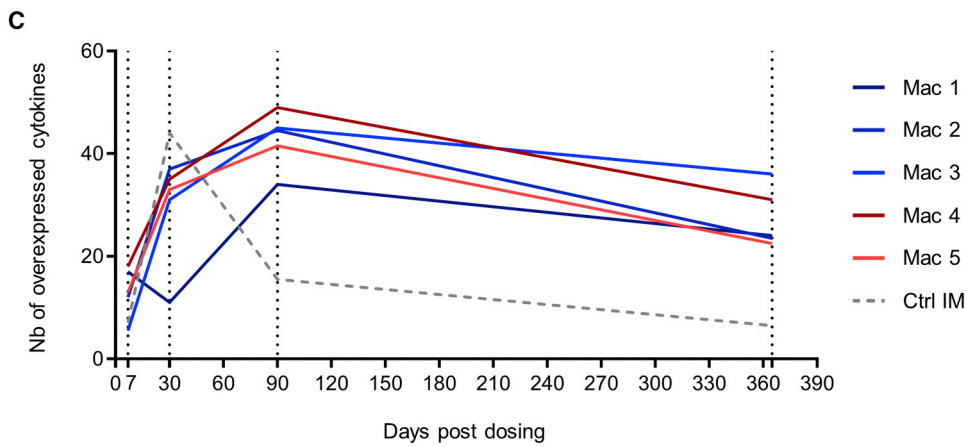
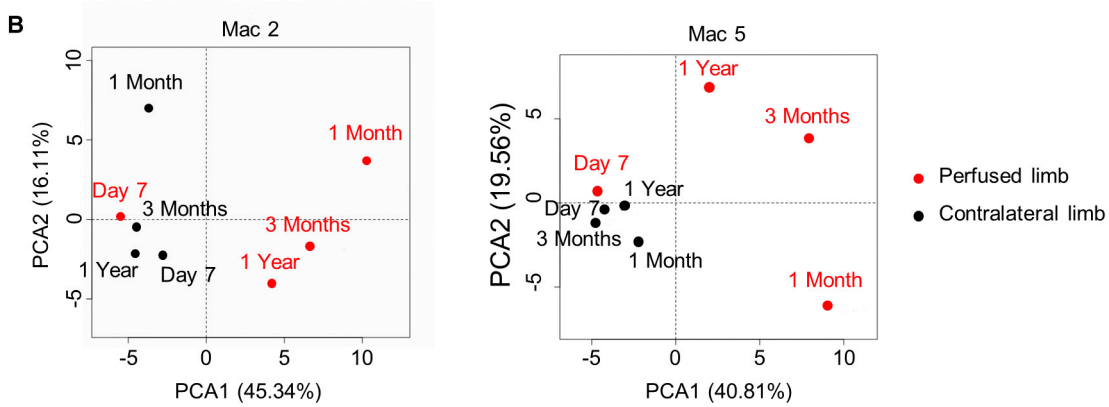
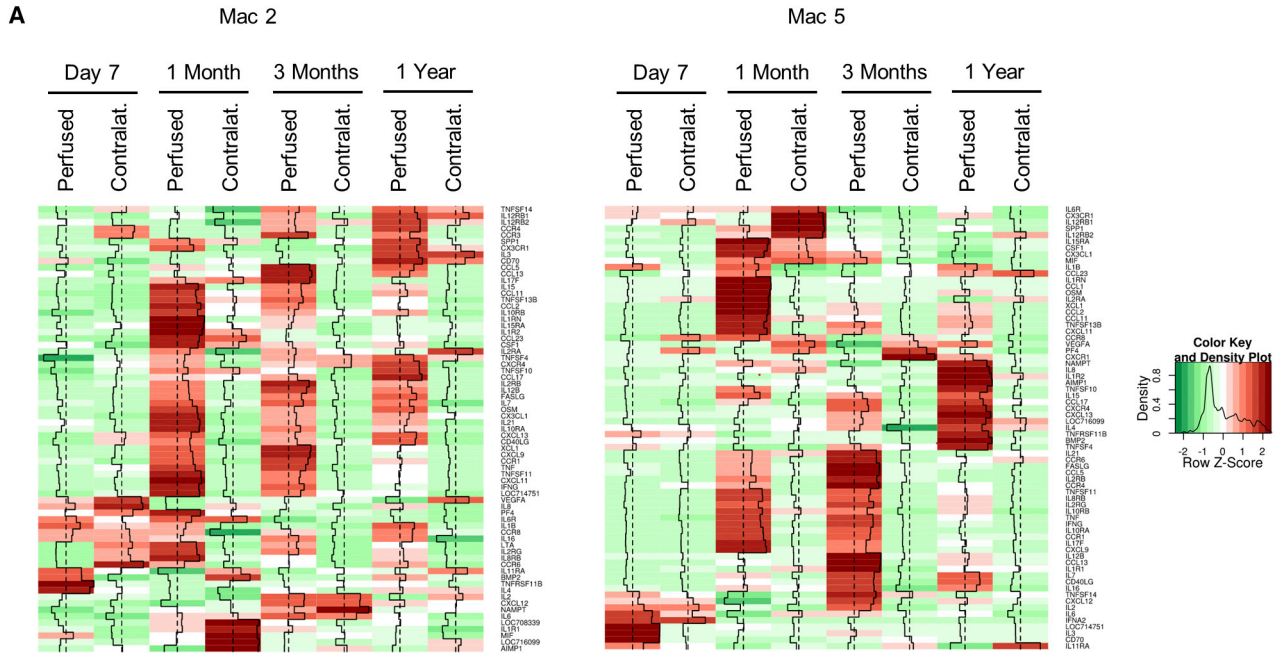


Figure 4. Regulatory T cells infiltrate the muscle after AAV8 LR delivery

Nonhuman primates were injected LR with a scAAV8-Des-GFP (Mac 1–3) or a scAAV8-CMV-GFP vector (Mac 4, 5; 7×10^{12} vg/kg). Muscles were harvested at necropsy. Detection of regulatory T cells (CD4+FoxP3+ cells) by immunohistochemistry in the perfused limb is shown. Scale bar: 50 μ m.



(legend on next page)

regenerating fiber differentiation and could therefore explain the presence of these regenerating centranucleated fibers 1 year post-injection.⁶⁹

Finally, persisting transgene expression in our model may not be related to the LR mode of delivery only but also to the AAV vector *per se*. In contrast to adenoviral vectors, for example, *in vivo* rAAV delivery was shown to be associated to tolerance to the viral capsid in humans⁴¹ and to the transgene product in animal models⁷⁰ in absence of any immune-suppressive regimen. In clinical trials, immune-suppressive drugs are generally transiently administered to prevent a potential reactivation of pre-existing anti-AAV immune responses. The choice of such regimen is crucial, as it can have an impact on T cell subtypes, including T-reg cells that could naturally induce *in vivo* tolerance to the vector and its product. As illustrated by Mingozzi et al.⁷¹ in a NHP model, the administration of a combination of three immune-suppressive drugs (mycophenolate mofetil (MMF), sirolimus, and daclizumab) led to a dramatic drop of Treg percentage and a boosting effect on B cell response with the detection of higher titers of anti-AAV2 antibodies, compared to monkeys receiving no immune-suppressive regimen or only MMF and sirolimus treatment. This was explained by the fact that daclizumab is an antagonist of the CD25 receptor, which is highly expressed on Tregs.

In conclusion, we confirm that LR delivery of an AAV vector with immunogenic properties leads to persisting transgene expression in the absence of any immune-suppressive regimen. Interestingly, GFP expression mediated by the CMV promoter led to higher transgene expression compared with the muscle-specific promoter but did not result in a higher immunogenicity. The inflammatory signals delivered *in situ*, and likely caused by the exogenous transgene product itself (e.g., GFP), were not sufficient to induce a deleterious immune response that would result in tissue damage. More importantly, these signals may participate in the recruitment of Tregs *in situ*. Induction of Treg-mediated immune modulation after LR delivery might be of particular interest for the treatment of patients with null mutations or patients with pre-existing cellular response to the transgene product.⁸ Finally, this administration route could be an alternative to IM or i.v. deliveries that are already used in clinics and which present limitations, such as transduction of limited areas and/or deleterious anti-capsid immune responses. Further investigation on this last aspect in reliable predictive animal models will be necessary, but this study further confirms that the LR route could be an alternative route of choice for AAV-mediated expression of therapeutic secreted factors from the skeletal muscle.

MATERIALS AND METHODS

A large part of this work was performed under the control of a quality management system that is approved by Lloyd's Register Quality Assurance LRQA to meet requirements of international Management System Standards ISO 9001:2008. It has been implemented to cover all activities in the laboratory, including research experiments and production of research-grade viral vectors.

Vector production

scAAV8 vectors were produced by the Center for Production of Vectors (CPV-vector core from University Hospital of Nantes/French Institute of Health [INSERM], University of Nantes [<https://umr1089.univ-nantes.fr/en/facilities-cores>]). Vectors were produced by cotransfection of human embryonic kidney (HEK) 293 cells with plasmid vectors carrying the GFP sequence driven by either the desmin promoter or the CMV promoter, a SV40 polyadenylation signal, and flanked by two AAV2-ITRs and the pDP8 helper plasmid containing viral sequences required for replication and encapsidation. Vectors were purified by cesium-chloride gradient, and titers were determined by dot plot and qPCR analysis to provide the number of vg per milliliter (vg/mL).

Animal care and welfare

All the animal work was done under the approval of the Institutional Animal Care and Use Committee of the University of Nantes and under the supervision of a Doctor of Veterinary Medicine Degree (DVM). Experiments were performed on 3.5–6.5 kg male cynomolgus monkeys (*Macaca fascicularis*) provided by BioPrim (Baziège, France). Cynomolgus monkeys seronegative for AAV8 were selected. All blood samples were collected under 20 µg/kg medetomidine (Domitor; Pfizer, Paris, France) associated to 8 mg/kg of ketamine (Imalgène; Rhône Mérieux, Toulouse, France). Surgical muscle biopsies were performed under ketamine (0.1 mL/kg)/medetomidine (0.01–0.04 mL/kg)-induced anesthesia; meloxicam (1 graduation/kg) was administered for the following 3–5 days to avoid discomfort. The animals were euthanized between 9 and 13 months after AAV injection; blood and tissues were collected for evaluation.

Vector administration

Six macaques were distributed in 2 groups (n = 3 per group). All the animals were injected by LR i.v. perfusion. Three monkeys received a scAAV8-desmin-GFP vector, and 3 monkeys received a scAAV8-CMV-GFP vector. The LR i.v. perfusion protocol was adapted from Su et al.⁷² Briefly, the vector was diluted in a ringer-lactate solution. The volume injected was about 20% of the limb volume (around 12 mL/kg). A cannulation was placed in the saphenous vein with a catheter, and a tourniquet was placed transmuscularly at the coxo-

Figure 5. Long-term expression of inflammatory genes in the perfused limb after AAV8 delivery

Nonhuman primates were injected LR with a scAAV8-Des-GFP (n = 3) or a scAAV8-CMV-GFP vector (n = 3; 7e12 vg/kg). Muscles from perfused limb and contralateral limb were harvested at day 7, day 30, day 60, and day 90 after dosing and at necropsy. (A) Representative heatmap of inflammatory gene expression determined by qRT-PCR and calculated from pairwise Pearson distances is shown. (B) Projection of qRT-PCR results in the individual space of principal-component analysis (PCA). Each illustration is representative of each group. (C) Quantification of overexpressed cytokines projected at more than 80% on the PCA1 and PCA2 axis from variable space for each monkey is shown. Ctrl IM, control monkey injected IM with a scAAV8-CMV-GFP vector (7e12 vg/kg).

Table 3. List of genes overexpressed over time after LR delivery

	ID code	Name	Description
Chemokines	CCL5/RANTES	chemokine (C-C motif) ligand 5	chemoattractant for blood monocytes, memory T helper cells, and eosinophils
	CXCL9/MIG	chemokine (C-X-C motif) ligand 9	chemoattractant for lymphocytes, involved in T cell trafficking
	XCL1/LTN	chemokine (C motif) ligand	specific chemotactic for T cells
	CXCL11/MIG	chemokine (C-X-C motif) ligand 11	chemoattractant for T cells
	CCL11/SCYA11	chemokine (C-C motif) ligand 11	chemotactic for eosinophil
	CXCL13/BLC	chemokine (C-X-C motif) ligand 13	chemoattractant for B cells, migration of B cells
	CCL2/MCP1	chemokine (C-C motif) ligand 2	recruitment of monocyte, memory T cells, and dendritic cells to inflammation sites
Cytokines	IFN- γ	interferon gamma	pleiotropic, trigger of cellular response
	IL-15	interleukin-15	regulation of T and NK activation and proliferation
	IL-7	interleukin-7	involved in B and T cell development
	IL-16/LCF	interleukin-16	pleiotropic, chemoattractant, modulator of T cell activation, recruits CD4 T cells and binds CD4 receptor
	TNF/TNFA	tumor necrosis factor	pleiotropic proinflammatory cytokine
	TNFSF11/RANKL	tumor necrosis factor superfamily member 11	cell survival factor for DC and regulation of T-cell-dependent immune response
	TNFSF13B/BAFF	tumor necrosis factor superfamily member 13	involved in proliferation and differentiation of B lymphocytes
Ligands and receptors	CD40LG/CD154	CD40 ligand	regulation of B cell function by engaging CD40 on the B cell surface
	FASLG/CD178	Fas ligand (TNF superfamily, member 6)	induction of apoptosis by binding to FAS
	IL-2RB/CD122	interleukin-2 receptor, beta chain	receptor-mediated endocytosis and transduction of mitogenic signals from IL-2
	IL-2RG/CD132	interleukin-2 receptor, gamma chain	involved in transduction of mitogenic signals from IL-2
	IL-8RB/CXCR2	interleukin-8 receptor, beta	mediation of neutrophil migration to sites of inflammation
	IL-10RA/CD210	interleukin-10 receptor subunit alpha	mediation of IL-10 signal and inhibition of proinflammatory cytokine synthesis
	IL-10RB/CDW210B	interleukin-10 receptor subunit beta	mediation of IL-10 signal and inhibition of proinflammatory cytokine synthesis

femoral articulation. The injection started after 10 min of an ischemic period and was performed with a delivery pressure of 300 mm Hg. After injection, transvenular extravasation of the vector was maintained 10 min before releasing the tourniquet. One control monkey (Ctrl IM) was injected IM. The IM injection consisted of an injection of 7e12 vg/kg of the scAAV8-CMV-GFP vector over 5 pretattooed injection sites along the tibialis anterior muscle.

Vector biodistribution

Genomic DNA (gDNA) was isolated from tissues using Gentra Pure-gene kit (QIAGEN) according to the manufacturer's recommendations. Vector biodistribution was determined by qPCR using 50 ng of gDNA as an input and by targeting the GFP sequence with the following primers: forward primer: 5'-ACTACAACAGCCA CAACGTCTATATCA-3', reverse primer 5'-GGCGGATCTT

GAAGTTCACC-3', and probe 5' (6 FAM)-3' TAMRA CCG ACA AGC AGA ACG GCA TCA. The ϵ -globin sequence was used as a reference gene and quantified using the following primers: forward primer: 5'-ACATAGCTTGCTTCAGAACGGT-3'; reverse primer: 5'-AGTGTCTTCATCCTGCCCTAAA-3'; and probe: 5' (6 FAM)-3' TAMRA TGCAGGCTGCCTGGCAGAAGC. Quantification was performed using the StepOne Plus Reader (Applied Biosystem, Thermo Fisher Scientific). For each sample, Ct values were compared with those obtained with linearized plasmid standard dilutions carrying either the GFP sequence or the ϵ -globin sequences.

Histopathological analysis and immunostaining

HPS staining

Skeletal muscle paraffin sections (5 μ m) were collected on slides. HPS staining was performed as per standard histological protocols using

formalin-fixed and paraffine-embedded muscle sections. The slides were observed using a Hamamatsu NanoZoomer (Bacus Laboratories, Chicago, IL, USA) and analyzed using the NDP.View2 analyze software.

GFP staining and immunohistochemistry

Tissues were either fixed in 10% neutral-buffered formalin, processed, and embedded in paraffin or were frozen in isopentane cooled in liquid nitrogen. Tissues were cut into 5- μ m sections. Immunohistochemical staining for GFP+ cells and Tregs (CD3+CD4+FoxP3+) were performed on paraffin-embedded sections, whereas immunohistochemical staining for CD4 and CD8 T cells (CD3+CD4+ and CD3+CD8+, respectively) were performed on frozen sections. Paraffin tissue sections were deparaffinized, rehydrated, and then antigen was unmasked by boiling the section in ready-to-use citrate-based pH 6.0. Skeletal muscle cryosections were collected on slides, air-dried, and fixed with 4% paraformaldehyde (PFA) (Thermo Scientific) for 10 min. All the sections were permeabilized in PBS containing 0.2% Triton X-100 for 10 min at room temperature (RT). Non-specific activity was blocked by incubating the sections for 45 min at RT in 10% NHP serum, 2% goat serum in PBS, and 5% BSA in PBS. Sections were incubated overnight at 4°C in primary antibody diluted in PBS. Monoclonal rabbit anti-GFP (1:100; 632380; Clontech Laboratories), monoclonal rabbit anti-human CD3 (1:200; ab11089; Abcam), monoclonal rabbit anti-human CD4 (1:200; ab133616; Abcam), and monoclonal mouse anti-human FoxP3 (1:50; 14-4777; eBioscience) antibodies were used to detect GFP+ cells and Tregs. Polyclonal rabbit anti-human CD3 (A0452; Dako), monoclonal mouse anti-human CD4 (317402; BioLegend), and monoclonal rat anti-human CD8 (MCA351GT; Serotec) antibodies were used to detect CD4 and CD8 T cells. After washing with PBS, sections were incubated with goat anti-rabbit Alexa-488-conjugated antibody (1:300; A11034; Life Technologies), goat anti-mouse Alexa-Fluor-647-conjugated antibody (1:300; A21240; Life Technologies), and/or goat anti-rat Alexa-Fluor-555-conjugated antibody (1:300; A21434; Life Technologies) for 1 h at RT. Nuclei were counterstained with DAPI (1:500; Sigma), and the slides were mounted in Prolong Gold anti-fade reagent (Life Technologies). Slides were examined using a laser scanning confocal microscope (Nikon A1RSi). Images were merged using Fiji software (National Institute of Health, Bethesda, MD, USA).

Anti-GFP immune response analysis

Humoral immune response

Serum was collected prior to dose; at day 7, day 15, day 30, day 60, day 90, and month 6 post-injection; and at necropsy. Anti-GFP antibodies were detected by enzyme-linked immunosorbent assay (ELISA). Plates were coated with 2 μ g/mL of recombinant GFP (Millipore) in 0.1M carbonate coating buffer at 4°C overnight. The plates were blocked with PBS-Tween 0.1% gelatin 1% at 37°C. Monkey sera were serially diluted and incubated for 2 h at 37°C. The positive control consisted of a commercial anti-GFP antibody (Millipore). Plates were then incubated with a goat anti-rhesus IgG horseradish peroxi-

dase (HRP) antibody (Southern Biotech) for 1 h at 37°C. Substrate (tetramethylbenzidine [TMB]; BD Biosciences) was added, and plates were incubated for 5 min at RT. The reaction was stopped using 1M phosphoric acid. Plates were read in a spectrometer (Multiscan GO; Thermo Fisher Scientific) at 450 nm with a correction at 570 nm. Threshold of positivity was determined using 22 negative sera obtained from naive macaques as mean of optic density (OD) for each dilution + 2*SD. IgG titers for experimental animals were defined as the last serum dilution for which OD remained above the threshold.

Cellular immune response

The anti-GFP immune cellular response analysis was performed using an ELISpot assay to measure IFN- γ and IL-2 secretion in PBMCs isolated prior to dose and at necropsy and, in total splenocytes and CD4- or CD8-depleted splenocytes collected at day 60 post-injection. CD4+ and CD8+ T cells were depleted by positive selection using Special StemSep Rhesus CD4+ or CD8+ Tetramer kits (STEMCELL Technologies). Cell depletion efficiency was determined by flow cytometry before (total splenocytes) and after magnetic separation (CD4- and CD8-depleted splenocytes). Briefly, CD4+ T cell and CD8+ T cell populations were analyzed using CD3 (557749; BD Biosciences)/CD4 (556616; BD Biosciences) and CD3/CD8 (301035; BioLegend) markers, respectively. Extracellular staining consisted of cell incubation on ice for 30 min. Cells were then washed twice with 1 \times PBS and re-suspended in 1 \times PBS supplemented with 0.5% fetal bovine serum (FBS) and 2 mM EDTA. Cells were acquired using a BD FACS LSRII flow cytometer (BD Biosciences) and analyzed with FlowJo software (v.10; BD Biosciences). IFN- γ (MABTech) and IL-2 (Ucytech) ELISpot assays were performed according to the manufacturer's recommendations (Monkey IFN- γ ELISpot^{PLUS} kit; MABTech). Briefly, cells were stimulated *in vitro* for 48 h with overlapping peptides spanning the GFP sequence and divided into 5 pools (10 μ g/mL; 15 mers overlapping by 10 amino acids [aas]; Sigma). A negative control consisted of unstimulated cells (medium only), whereas PMA (10 ng/mL)/ionomycin (250 ng/mL) stimulation was used as a positive control for cytokine secretion. Spot number was determined using an ELISpot reader ELR07 (AID) and analyzed with AID ELISpot Reader Software V7.0. Responses were considered positive when the number of spot-forming colonies (SFCs) per 1e6 cells was >50 and at least 3-fold higher than the control condition. AAV capsid cellular immune response was evaluated using the same IFN- γ ELISpot method but using an overlapping peptide library spanning the VP1 capsid protein sequence and divided into 3 pools for T cell stimulation.

Quantification and analysis of inflammatory gene expression

Frozen tissue was homogenized in TRIzol (Life Technologies), and total RNA was isolated according to the manufacturer's instructions. Total RNA was treated with RNase-Free DNase Set (QIAGEN) to eliminate DNA contamination. Then RNAs were concentrated using the RNeasy MinElute Cleanup kit (QIAGEN). Reverse-transcription reactions on 300 ng of total RNA from muscles was performed using the RT2 First Strand kit (QIAGEN). 84 genes involved in

inflammatory response were analyzed using RT2 Profiler Rhesus Macaque Inflammatory Cytokines & Receptors PCR Array (QIAGEN). RQ values ($2^{-\Delta Ct}$) were calculated using the dedicated Web-based software (<https://geneglobe.qiagen.com/fr/products/analysis-type/analysis-type-pcr/pcr-rna-lncrna/>). Raw RQ values and open-source R script for heatmap and PCA are available at <https://github.com/ashslide/TaqMDA> together with a detailed online documentation. N/A values correspond to undetected or reliable expression of genes. To minimize stochasticity, a max percentage of N/A values was fixed at 80%.

Statistical analysis

Statistical analyses were performed with GraphPad Prism, version 8.0 (GraphPad Software). Each macaque was compared to the others using the Mann-Whitney non-parametric statistical test. Differences were considered significant at a $p < 0.05$.

SUPPLEMENTAL INFORMATION

Supplemental Information can be found online at <https://doi.org/10.1016/j.omtm.2021.02.003>.

ACKNOWLEDGMENTS

The authors thank the Oniris Boisbonne Centre (Nantes, France) for NHP housing and care, the Center for Production of Vectors (CPV-vector core from the University Hospital of Nantes/French Institute of Health [INSERM]/University of Nantes) for providing rAAV2/8 vectors (<https://umr1089.univ-nantes.fr/en/facilities-cores>), and Lydie Guigand, Maëva Dutilleul, and Héclicia Goubin from the UMR703 (Oniris, Nantes, France) for their help with tissue preparation. The authors would also like to acknowledge the Cellular and Tissular Imaging Core Facility (MicroPICell; <https://micropicell.univ-nantes.fr>) and the Cytometry Facility Cytocell (Cytocell; <https://cytocell.univ-nantes.fr/>) at the University of Nantes for expert technical assistance. The study received funding from the Inserm; the CHU de Nantes; the “Fondation pour la Therapie Genique en Pays de Loire”; the AFM-Téléthon (Association Française contre les Myopathies); the National Research Agency (ANR-09-BLAN-0265 GENETOL program; ANR-17-CE17-0007-01 TOLGEN program); the “Region Pays de La Loire” in the context of IMBIO-DC consortium; and the IHU-Cesti project that received French government financial support managed by the National Research Agency (ANR-10-IBHU-005 program). The IHU-Cesti project was also supported by Nantes Metropole and Région Pays de la Loire. G.G. was funded by the French Ministry of Research (PhD MRT fellowship). This work was performed at INSERM UMR1089, Nantes, France.

AUTHOR CONTRIBUTIONS

Conceptualization, G.G., M.G., P.M., and O.A.; methodology, G.G., M.G., J.-Y.D., C.L.G., P.M., Y.C., and O.A.; investigation, G.G., M.G., M.D., M.J., V.P., N.J., and J.L.D.; formal analysis, A.L. and M.G.; writing – original draft, G.G., M.G., and O.A.; writing – review & editing, G.G., M.G., and O.A.; supervision, P.M., Y.C., and O.A.

DECLARATION OF INTERESTS

G.G., M.G., M.D., N.J., V.P., M.J., A.L., J.L.D., J.-Y.D., C.L.G., P.M., Y.C., and O.A. declare no competing interests. P.M. is an employee of Asklepios BioPharmaceutical.

REFERENCES

- Al-Zaidy, S.A., Kolb, S.J., Lowes, L., Alfano, L.N., Shell, R., Church, K.R., Nagendran, S., Sproule, D.M., Feltner, D.E., Wells, C., et al. (2019). AVXS-101 (Onasemnogene Apeparovvec) for SMA1: comparative study with a prospective natural history cohort. *J. Neuromuscul. Dis.* 6, 307–317.
- Maguire, A.M., Russell, S., Wellman, J.A., Chung, D.C., Yu, Z.-F., Tillman, A., Wittes, J., Pappas, J., Elci, O., Marshall, K.A., et al. (2019). Efficacy, safety, and durability of voretigene neparovvec-rzyl in RPE65 mutation-associated inherited retinal dystrophy: results of phase 1 and 3 trials. *Ophthalmology* 126, 1273–1285.
- Gaudet, D., Méthot, J., Déry, S., Brisson, D., Essiembre, C., Tremblay, G., Tremblay, K., de Wal, J., Twisk, J., van den Bulk, N., et al. (2013). Efficacy and long-term safety of alipogene tiparovvec (AAV1-LPLS447X) gene therapy for lipoprotein lipase deficiency: an open-label trial. *Gene Ther.* 20, 361–369.
- Wang, B., Li, J., and Xiao, X. (2000). Adeno-associated virus vector carrying human minidystrophin genes effectively ameliorates muscular dystrophy in mdx mouse model. *Proc. Natl. Acad. Sci. USA* 97, 13714–13719.
- Bowles, D.E., McPhee, S.W.J., Li, C., Gray, S.J., Samulski, J.J., Camp, A.S., Li, J., Wang, B., Monahan, P.E., Rabinowitz, J.E., et al. (2012). Phase 1 gene therapy for Duchenne muscular dystrophy using a translational optimized AAV vector. *Mol. Ther.* 20, 443–455.
- Mendell, J.R., Rodino-Klapac, L.R., Rosales-Quintero, X., Kota, J., Coley, B.D., Galloway, G., Craenen, J.M., Lewis, S., Malik, V., Shilling, C., et al. (2009). Limb-girdle muscular dystrophy type 2D gene therapy restores alpha-sarcoglycan and associated proteins. *Ann. Neurol.* 66, 290–297.
- Mendell, J.R., Rodino-Klapac, L.R., Rosales, X.Q., Coley, B.D., Galloway, G., Lewis, S., Malik, V., Shilling, C., Byrne, B.J., Conlon, T., et al. (2010). Sustained alpha-sarcoglycan gene expression after gene transfer in limb-girdle muscular dystrophy, type 2D. *Ann. Neurol.* 68, 629–638.
- Mendell, J.R., Campbell, K., Rodino-Klapac, L., Sahenk, Z., Shilling, C., Lewis, S., Bowles, D., Gray, S., Li, C., Galloway, G., et al. (2010). Dystrophin immunity in Duchenne’s muscular dystrophy. *N. Engl. J. Med.* 363, 1429–1437.
- Kay, M.A., Manno, C.S., Ragni, M.V., Larson, P.J., Couto, L.B., McClelland, A., Glader, B., Chew, A.J., Tai, S.J., Herzog, R.W., et al. (2000). Evidence for gene transfer and expression of factor IX in haemophilia B patients treated with an AAV vector. *Nat. Genet.* 24, 257–261.
- Manno, C.S., Chew, A.J., Hutchison, S., Larson, P.J., Herzog, R.W., Arruda, V.R., Tai, S.J., Ragni, M.V., Thompson, A., Ozelo, M., et al. (2003). AAV-mediated factor IX gene transfer to skeletal muscle in patients with severe hemophilia B. *Blood* 101, 2963–2972.
- Brantly, M.L., Spencer, L.T., Humphries, M., Conlon, T.J., Spencer, C.T., Poirier, A., Garlington, W., Baker, D., Song, S., Berns, K.I., et al. (2006). Phase I trial of intramuscular injection of a recombinant adeno-associated virus serotype 2 alpha1-antitrypsin (AAT) vector in AAT-deficient adults. *Hum. Gene Ther.* 17, 1177–1186.
- Arruda, V.R., Schuettrumpf, J., Herzog, R.W., Nichols, T.C., Robinson, N., Lotfi, Y., Mingozzi, F., Xiao, W., Couto, L.B., and High, K.A. (2004). Safety and efficacy of factor IX gene transfer to skeletal muscle in murine and canine hemophilia B models by adeno-associated viral vector serotype 1. *Blood* 103, 85–92.
- Mingozzi, F., Meulenberg, J.J., Hui, D.J., Basner-Tschakarjan, E., Hasbrouck, N.C., Edmonson, S.A., Hutnick, N.A., Betts, M.R., Kastelein, J.J., Stroes, E.S., and High, K.A. (2009). AAV-1-mediated gene transfer to skeletal muscle in humans results in dose-dependent activation of capsid-specific T cells. *Blood* 114, 2077–2086.
- Flotte, T.R., Trapnell, B.C., Humphries, M., Carey, B., Calcedo, R., Rouhani, F., Campbell-Thompson, M., Yachnis, A.T., Sandhaus, R.A., McElvaney, N.G., et al. (2011). Phase 2 clinical trial of a recombinant adeno-associated viral vector expressing $\alpha 1$ -antitrypsin: interim results. *Hum. Gene Ther.* 22, 1239–1247.

15. Schneider, J., Gonzalez, J., Brown, K., Golebiowski, D., Ricotti, V., Quiroz, J., and Morris, C. (2017). SGT-001 Micro-dystrophin gene therapy for Duchenne muscular dystrophy. *Neuromuscul. Disord.* 27, S188.
16. Mendell, J.R., Sahenk, Z., Lehman, K., Nease, C., Lowes, L.P., Miller, N.F., Iammarino, M.A., Alfano, L.N., Nicholl, A., Al-Zaidy, S., et al. (2020). Assessment of systemic delivery of rAAVrh74.MHCK7.micro-dystrophin in children with Duchenne muscular dystrophy: a nonrandomized controlled trial. *JAMA Neurol.* 77, 1122–1131.
17. Pfizer. (2020). Pfizer's new phase 1b results of gene therapy in ambulatory boys with Duchenne muscular dystrophy (DMD) support advancement into pivotal phase 3 study, <https://investors.pfizer.com/investor-news/press-release-details/2020/Pfizers-New-Phase-1b-Results-of-Gene-Therapy-in-Ambulatory-Boys-with-Duchenne-Muscular-Dystrophy-DMD-Support-Advancement-into-Pivotal-Phase-3-Study/default.aspx>.
18. Adis Insight (2021). ASPIRO: a phase 1/2, randomized, open-label, ascending-dose, delayed-treatment concurrent control clinical study to evaluate the safety and efficacy of AT132, an AAV8-delivered gene therapy in X-linked myotubular myopathy (XLMTM) patients, https://idp.springer.com/authorize?client_id=adis&redirect_uri=https%3A%2F%2Fadisinsight.springer.com%2Ftrials%2F700275939&response_type=cookie.
19. Hinderer, C., Katz, N., Buza, E.L., Dyer, C., Goode, T., Bell, P., Richman, L.K., and Wilson, J.M. (2018). Severe toxicity in nonhuman primates and piglets following high-dose intravenous administration of an adeno-associated virus vector expressing human SMN. *Hum. Gene Ther.* 29, 285–298.
20. (2020). High-dose AAV gene therapy deaths. *Nat. Biotechnol.* 38, 910.
21. Duan, D. (2018). Micro-dystrophin gene therapy goes systemic in Duchenne muscular dystrophy patients. *Hum. Gene Ther.* 29, 733–736.
22. Arruda, V.R., Stedman, H.H., Nichols, T.C., Haskins, M.E., Nicholson, M., Herzog, R.W., Couto, L.B., and High, K.A. (2005). Regional intravascular delivery of AAV-2-F.IX to skeletal muscle achieves long-term correction of hemophilia B in a large animal model. *Blood* 105, 3458–3464.
23. Toromanoff, A., Chérel, Y., Guilbaud, M., Penaud-Budloo, M., Snyder, R.O., Haskins, M.E., Deschamps, J.-Y., Guigand, L., Podevin, G., Arruda, V.R., et al. (2008). Safety and efficacy of regional intravenous (r.i.) versus intramuscular (i.m.) delivery of rAAV1 and rAAV8 to nonhuman primate skeletal muscle. *Mol. Ther.* 16, 1291–1299.
24. Le Guiner, C., Montus, M., Servais, L., Chérel, Y., François, V., Thibaud, J.-L., Wary, C., Matot, B., Larcher, T., Guigand, L., et al. (2014). Forelimb treatment in a large cohort of dystrophic dogs supports delivery of a recombinant AAV for exon skipping in Duchenne patients. *Mol. Ther.* 22, 1923–1935.
25. Toromanoff, A., Adjali, O., Larcher, T., Hill, M., Guigand, L., Chenuaud, P., Deschamps, J.-Y., Gauthier, O., Blancho, G., Vanhove, B., et al. (2010). Lack of immunotoxicity after regional intravenous (RI) delivery of rAAV to nonhuman primate skeletal muscle. *Mol. Ther.* 18, 151–160.
26. Guilbaud, M., Devaux, M., Couzinié, C., Le Duff, J., Toromanoff, A., Vandamme, C., Jaulin, N., Gernoux, G., Larcher, T., Moullier, P., et al. (2019). Five years of successful inducible transgene expression following locoregional adeno-associated virus delivery in nonhuman primates with no detectable immunity. *Hum. Gene Ther.* 30, 802–813.
27. Fan, Z., Kocis, K., Valley, R., Howard, J.F., Chopra, M., An, H., Lin, W., Muenzer, J., and Powers, W. (2012). Safety and feasibility of high-pressure transvenous limb perfusion with 0.9% saline in human muscular dystrophy. *Mol. Ther.* 20, 456–461.
28. Gruntman, A.M., Gernoux, G., Tang, Q., Ye, G.-J., Knop, D.R., Wang, G., Benson, J., Coleman, K.E., Keeler, A.M., Mueller, C., et al. (2019). Bridging from intramuscular to limb perfusion delivery of rAAV: optimization in a non-human primate study. *Mol. Ther. Methods Clin. Dev.* 13, 233–242.
29. Haurigot, V., Mingozzi, F., Buchlis, G., Hui, D.J., Chen, Y., Basner-Tschakarjan, E., Arruda, V.R., Radu, A., Franck, H.G., Wright, J.F., et al. (2010). Safety of AAV factor IX peripheral transvenous gene delivery to muscle in hemophilia B dogs. *Mol. Ther.* 18, 1318–1329.
30. Rodino-Klapac, L.R., Montgomery, C.L., Bremer, W.G., Shontz, K.M., Malik, V., Davis, N., Sprinkle, S., Campbell, K.J., Sahenk, Z., Clark, K.R., et al. (2010). Persistent expression of FLAG-tagged micro dystrophin in nonhuman primates following intramuscular and vascular delivery. *Mol. Ther.* 18, 109–117.
31. Nathwani, A.C., Tuddenham, E.G.D., Rangarajan, S., Rosales, C., McIntosh, J., Linch, D.C., Chowdhury, P., Riddell, A., Pie, A.J., Harrington, C., et al. (2011). Adenovirus-associated virus vector-mediated gene transfer in hemophilia B. *N. Engl. J. Med.* 365, 2357–2365.
32. Martino, A.T., Suzuki, M., Markusic, D.M., Zolotukhin, I., Ryals, R.C., Moghimi, B., Ertl, H.C.J., Muruve, D.A., Lee, B., and Herzog, R.W. (2011). The genome of self-complementary adeno-associated viral vectors increases Toll-like receptor 9-dependent innate immune responses in the liver. *Blood* 117, 6459–6468.
33. Rogers, G.L., Martino, A.T., Zolotukhin, I., Ertl, H.C.J., and Herzog, R.W. (2014). Role of the vector genome and underlying factor IX mutation in immune responses to AAV gene therapy for hemophilia B. *J. Transl. Med.* 12, 25.
34. Gao, G., Wang, Q., Calcedo, R., Mays, L., Bell, P., Wang, L., Vandenbergh, L.H., Grant, R., Sanmiguel, J., Furth, E.E., and Wilson, J.M. (2009). Adeno-associated virus-mediated gene transfer to nonhuman primate liver can elicit destructive transgene-specific T cell responses. *Hum. Gene Ther.* 20, 930–942.
35. Wang, L., Calcedo, R., Wang, H., Bell, P., Grant, R., Vandenbergh, L.H., Sanmiguel, J., Morizono, H., Batshaw, M.L., and Wilson, J.M. (2010). The pleiotropic effects of natural AAV infections on liver-directed gene transfer in macaques. *Mol. Ther.* 18, 126–134.
36. Borel, F., Gernoux, G., Sun, H., Stock, R., Blackwood, M., Brown, R.H., Jr., and Mueller, C. (2018). Safe and effective superoxide dismutase 1 silencing using artificial microRNA in macaques. *Sci. Transl. Med.* 10, eaa6414.
37. Blattman, J.N., Grayson, J.M., Wherry, E.J., Kaech, S.M., Smith, K.A., and Ahmed, R. (2003). Therapeutic use of IL-2 to enhance antiviral T-cell responses in vivo. *Nat. Med.* 9, 540–547.
38. Pipkin, M.E., Sacks, J.A., Cruz-Guilloty, F., Lichtenheld, M.G., Bevan, M.J., and Rao, A. (2010). Interleukin-2 and inflammation induce distinct transcriptional programs that promote the differentiation of effector cytolytic T cells. *Immunity* 32, 79–90.
39. Gernoux, G., Gruntman, A.M., Blackwood, M., Zieger, M., Flotte, T.R., and Mueller, C. (2020). Muscle-directed delivery of an AAV1 vector leads to capsid-specific T cell exhaustion in nonhuman primates and humans. *Mol. Ther.* 28, 747–757.
40. Mays, L.E., Wang, L., Lin, J., Bell, P., Crawford, A., Wherry, E.J., and Wilson, J.M. (2014). AAV8 induces tolerance in murine muscle as a result of poor APC transduction, T cell exhaustion, and minimal MHCI upregulation on target cells. *Mol. Ther.* 22, 28–41.
41. Mueller, C., Chulay, J.D., Trapnell, B.C., Humphries, M., Carey, B., Sandhaus, R.A., McElvaney, N.G., Messina, L., Tang, Q., Rouhani, F.N., et al. (2013). Human Treg responses allow sustained recombinant adeno-associated virus-mediated transgene expression. *J. Clin. Invest.* 123, 5310–5318.
42. Manno, C.S., Pierce, G.F., Arruda, V.R., Glader, B., Ragni, M., Rasko, J.J.E., Ozelo, M.C., Hoots, K., Blatt, P., Konkle, B., et al. (2006). Successful transduction of liver in hemophilia by AAV-Factor IX and limitations imposed by the host immune response. *Nat. Med.* 12, 342–347.
43. Mingozzi, F., Maus, M.V., Hui, D.J., Sabatino, D.E., Murphy, S.L., Rasko, J.E.J., Ragni, M.V., Manno, C.S., Sommer, J., Jiang, H., et al. (2007). CD8(+) T-cell responses to adeno-associated virus capsid in humans. *Nat. Med.* 13, 419–422.
44. Calcedo, R., Somanathan, S., Qin, Q., Betts, M.R., Rech, A.J., Vonderheide, R.H., Mueller, C., Flotte, T.R., and Wilson, J.M. (2017). Class I-restricted T-cell responses to a polymorphic peptide in a gene therapy clinical trial for α -1-antitrypsin deficiency. *Proc. Natl. Acad. Sci. USA* 114, 1655–1659.
45. Mendell, J.R., Al-Zaidy, S., Shell, R., Arnold, W.D., Rodino-Klapac, L.R., Prior, T.W., Lowes, L., Alfano, L., Berry, K., Church, K., et al. (2017). Single-dose gene-replacement therapy for spinal muscular atrophy. *N. Engl. J. Med.* 377, 1713–1722.
46. Gernoux, G., Wilson, J.M., and Mueller, C. (2017). Regulatory and exhausted T cell responses to AAV capsid. *Hum. Gene Ther.* 28, 338–349.
47. Le Guiner, C., Servais, L., Montus, M., Larcher, T., Fraysse, B., Moullier, S., Allais, M., François, V., Dutilleul, M., Malerba, A., et al. (2017). Long-term microdystrophin gene therapy is effective in a canine model of Duchenne muscular dystrophy. *Nat. Commun.* 8, 16105.
48. Ferreira, V., Twisk, J., Kwikkers, K., Aronica, E., Brisson, D., Methot, J., Petry, H., and Gaudet, D. (2014). Immune responses to intramuscular administration of alipogene tiparvec (AAV1-LPL(S447X)) in a phase II clinical trial of lipoprotein lipase deficiency gene therapy. *Hum. Gene Ther.* 25, 180–188.

49. Mount, J.D., Herzog, R.W., Tillson, D.M., Goodman, S.A., Robinson, N., McClelland, M.L., Bellinger, D., Nichols, T.C., Arruda, V.R., Lothrop, C.D., Jr., and High, K.A. (2002). Sustained phenotypic correction of hemophilia B dogs with a factor IX null mutation by liver-directed gene therapy. *Blood* *99*, 2670–2676.
50. Chulay, J.D., Ye, G.-J., Thomas, D.L., Knop, D.R., Benson, J.M., Hutt, J.A., Wang, G., Humphries, M., and Flotte, T.R. (2011). Preclinical evaluation of a recombinant adeno-associated virus vector expressing human alpha-1 antitrypsin made using a recombinant herpes simplex virus production method. *Hum. Gene Ther.* *22*, 155–165.
51. Pescatori, M., Broccolini, A., Minetti, C., Bertini, E., Bruno, C., D'amico, A., Bernardini, C., Mirabella, M., Silvestri, G., Giglio, V., et al. (2007). Gene expression profiling in the early phases of DMD: a constant molecular signature characterizes DMD muscle from early postnatal life throughout disease progression. *FASEB J.* *21*, 1210–1226.
52. Mojumdar, K., Liang, F., Giordano, C., Lemaire, C., Danialou, G., Okazaki, T., Bourdon, J., Rafei, M., Galipeau, J., Divangahi, M., and Petrof, B.J. (2014). Inflammatory monocytes promote progression of Duchenne muscular dystrophy and can be therapeutically targeted via CCR2. *EMBO Mol. Med.* *6*, 1476–1492.
53. Villalta, S.A., Rosenthal, W., Martinez, L., Kaur, A., Sparwasser, T., Tidball, J.G., Margeta, M., Spencer, M.J., and Bluestone, J.A. (2014). Regulatory T cells suppress muscle inflammation and injury in muscular dystrophy. *Sci. Transl. Med.* *6*, 258ra142.
54. Burzyn, D., Kuswanto, W., Kolodin, D., Shadrach, J.L., Cerletti, M., Jang, Y., Sefik, E., Tan, T.G., Wagers, A.J., Benoist, C., and Mathis, D. (2013). A special population of regulatory T cells potentiates muscle repair. *Cell* *155*, 1282–1295.
55. Rigamonti, E., Zordan, P., Sciorati, C., Rovere-Querini, P., and Brunelli, S. (2014). Macrophage plasticity in skeletal muscle repair. *BioMed Res. Int.* *2014*, 560629.
56. Schiaffino, S., Pereira, M.G., Ciciliot, S., and Rovere-Querini, P. (2017). Regulatory T cells and skeletal muscle regeneration. *FEBS J.* *284*, 517–524.
57. Sciorati, C., Rigamonti, E., Manfredi, A.A., and Rovere-Querini, P. (2016). Cell death, clearance and immunity in the skeletal muscle. *Cell Death Differ.* *23*, 927–937.
58. Duchesne, E., Dufresne, S.S., and Dumont, N.A. (2017). Impact of inflammation and anti-inflammatory modalities on skeletal muscle healing: from fundamental research to the clinic. *Phys. Ther.* *97*, 807–817.
59. Murai, M., Turovskaya, O., Kim, G., Madan, R., Karp, C.L., Cheroutre, H., and Kronenberg, M. (2009). Interleukin 10 acts on regulatory T cells to maintain expression of the transcription factor Foxp3 and suppressive function in mice with colitis. *Nat. Immunol.* *10*, 1178–1184.
60. Chaudhry, A., Samstein, R.M., Treuting, P., Liang, Y., Pils, M.C., Heinrich, J.-M., Jack, R.S., Wunderlich, F.T., Brüning, J.C., Müller, W., and Rudensky, A.Y. (2011). Interleukin-10 signaling in regulatory T cells is required for suppression of Th17 cell-mediated inflammation. *Immunity* *34*, 566–578.
61. Shouval, D.S., Biswas, A., Goettel, J.A., McCann, K., Conaway, E., Redhu, N.S., Mascanfroni, I.D., Al Adham, Z., Lavoie, S., Ibourk, M., et al. (2014). Interleukin-10 receptor signaling in innate immune cells regulates mucosal immune tolerance and anti-inflammatory macrophage function. *Immunity* *40*, 706–719.
62. Wang, Z., Hong, J., Sun, W., Xu, G., Li, N., Chen, X., Liu, A., Xu, L., Sun, B., and Zhang, J.Z. (2006). Role of IFN-gamma in induction of Foxp3 and conversion of CD4+ CD25- T cells to CD4+ Tregs. *J. Clin. Invest.* *116*, 2434–2441.
63. Chen, X., Wu, X., Zhou, Q., Howard, O.M.Z., Netea, M.G., and Oppenheim, J.J. (2013). TNFR2 is critical for the stabilization of the CD4+Foxp3+ regulatory T cell phenotype in the inflammatory environment. *J. Immunol.* *190*, 1076–1084.
64. Chen, X., Bäuml, M., Männel, D.N., Howard, O.M.Z., and Oppenheim, J.J. (2007). Interaction of TNF with TNF receptor type 2 promotes expansion and function of mouse CD4+CD25+ T regulatory cells. *J. Immunol.* *179*, 154–161.
65. Hamano, R., Huang, J., Yoshimura, T., Oppenheim, J.J., and Chen, X. (2011). TNF optimally activates regulatory T cells by inducing TNF receptor superfamily members TNFR2, 4-1BB and OX40. *Eur. J. Immunol.* *41*, 2010–2020.
66. Yamaguchi, T., Wing, J.B., and Sakaguchi, S. (2011). Two modes of immune suppression by Foxp3(+) regulatory T cells under inflammatory or non-inflammatory conditions. *Semin. Immunol.* *23*, 424–430.
67. Klatzmann, D., and Abbas, A.K. (2015). The promise of low-dose interleukin-2 therapy for autoimmune and inflammatory diseases. *Nat. Rev. Immunol.* *15*, 283–294.
68. Feghali, C.A., and Wright, T.M. (1997). Cytokines in acute and chronic inflammation. *Front. Biosci.* *2*, d12–d26.
69. Tidball, J.G. (2011). Mechanisms of muscle injury, repair, and regeneration. *Compr. Physiol.* *1*, 2029–2062.
70. Dobrzynski, E., and Herzog, R.W. (2005). Tolerance induction by viral in vivo gene transfer. *Clin. Med. Res.* *3*, 234–240.
71. Mingozzi, F., Hasbrouck, N.C., Basner-Tschakarjan, E., Edmonson, S.A., Hui, D.J., Sabatino, D.E., Zhou, S., Wright, J.F., Jiang, H., Pierce, G.F., et al. (2007). Modulation of tolerance to the transgene product in a nonhuman primate model of AAV-mediated gene transfer to liver. *Blood* *110*, 2334–2341.
72. Su, L.T., Gopal, K., Wang, Z., Yin, X., Nelson, A., Kozyak, B.W., Burkman, J.M., Mitchell, M.A., Low, D.W., Bridges, C.R., and Stedman, H.H. (2005). Uniform scale-independent gene transfer to striated muscle after transvenular extravasation of vector. *Circulation* *112*, 1780–1788.